

- Taketani T, Taki T, Shibuya N, Ito E, Kitazawa J, Terui K et al. (2002). The *HOXD11* gene is fused to the *NUP98* gene in acute myeloid leukemia with t(2;11)(q31;p15). *Cancer Res* **62**: 33–37.
- Taki T, Sako M, Tsuchida M, Hayashi Y. (1997). The t(11;16)(q23;p13) translocation in myelodysplastic syndrome fuses the *MLL* gene to the *CBP* gene. *Blood* **89**: 3945–3950.
- Taki T, Taniwaki M. (2006). Chromosomal translocations in cancer and their relevance for therapy. *Curr Opin Oncol* **18**: 62–68.
- Taniwaki M, Matsuda F, Jauch A, Nishida K, Takashima T, Tagawa S et al. (1994). Detection of 14q32 translocations in B-cell malignancies by *in situ* hybridization with yeast artificial chromosome clones containing the human IgH gene locus. *Blood* **83**: 2962–2969.
- Von Bergh AR, Beverloo HB, Rombout P, van Wering ER, van Weel MH, Beverstock GC et al. (2002). *LAF4*, an *AF4*-related gene, is fused to *MLL* in infant acute lymphoblastic leukemia. *Genes Chromosomes Cancer* **37**: 106–109.
- Wang J, Hoshino T, Redner RL, Kajigaya S, Liu JM. (1998). *ETO*, fusion partner in t(8;21) acute myeloid leukemia, represses transcription by interaction with the human N-CoR/mSin3/HDAC1 complex. *Proc Natl Acad Sci USA* **95**: 10860–10865.
- Weng AP, Ferrando AA, Lee W, Lee W, Morris IV JP, Silverman LB et al. (2004). Activating mutations of *NOTCH1* in human T cell acute lymphoblastic leukemia. *Science* **306**: 269–271.
- Yan M, Burel SA, Peterson LF, Kanbe E, Iwasaki H, Boyapati A et al. (2004). Deletion of an AML1-ETO C-terminal NcoR/SMRT-interacting region strongly induces leukemia development. *Proc Natl Acad Sci USA* **101**: 17186–17191.
- Zhang JG, Goldman JM, Cross NC. (1995). Characterization of genomic *BCR-ABL* breakpoints in chronic myeloid leukemia by PCR. *Br J Haematol* **90**: 138–146.
- Zhang Y, Emmanuel N, Kamboj G, Chen J, Shurafa M, Van Dyke DL et al. (2004). *PRDX4*, a member of the peroxidoredoxin family, is fused to *AML1 (RUNX1)* in an acute myeloid leukemia patient with a t(X;21)(p22;q22). *Genes Chromosomes Cancer* **40**: 365–370.

Supplementary Information accompanies the paper on the Oncogene website (<http://www.nature.com/onc>).

CURRENT TOPICS

小児腫瘍のグループスタディーと病理

藤本純一郎 堀江 弘

病理と臨床・別刷

2008 vol. 26 no. 9

東京／文光堂／本郷

小児腫瘍のグループスタディと病理

藤本純一郎*1 堀江 弘**2

はじめに

今から約6年前に各種難治性疾患に関わるエビデンス創出の基盤づくりのための公的研究費投入が開始された。それを受けて、小児がんについても標準的治療法開発を目指した取り組みが開始された。現在、我が国では小児がんの病型ごとの臨床研究グループがつかられ、統一治療プロトコールに基づく臨床試験などが実施されている。各研究グループには数十～200程度の医療施設が参加している。それらの組織体制は種々であるが、運営委員会や幹事会等の運営母体、プロトコール作成や研究立案を行う各種委員会、研究事務局、データセンター、中央診断システム等から構成されている。

上記の組織体制の中で、病理医が関与する場合は主として中央診断システムの部分である。その他、臨床研究グループにおける中央診断に関わる業務は様々で、病理診断以外に、遺伝子診断(増幅、欠失、変異、キメラ遺伝子発現等)、染色体診断、骨髄スメア等の形態診断、CT・MRI等画像診断、などが存在する。中央診断システムの役割は標準化された診断による試験参加適格性判定や治療層別化判定に関連する情報提供が基本であるが、一部では治療層別化に有用な新規マーカー開発研究や病態解明に結びつく基礎研究も行われる場合がある。病理中央診断については日本病理学会小児腫瘍組織分類委員会の委員の多くが関わってきた。

小児がんは稀少であり、年間の発生数が1,500～2,000程度と予想されることから、これらの症例を効率よく収集するシステムとしても臨床研究グループによる症例のリクルート、その中での中央診断システムは貴重である。また、診断後の余剰検体や研究用検体

を保存し、基礎研究の推進に活用する仕組みも確立中である。また、小児がんの年間発生数把握に関する取り組みも始まっている。我が国におけるがん登録に対する取り組みは甚だしく遅れており、小児がん登録についても言わずもがなの状況である。しかしながら上記の臨床研究の推進ならびに予後の著明な改善に伴い、小児がん登録の重要性が増している。

本稿ではこれらの取り組みの現状を紹介する。

I. 小児がん臨床研究グループの活動

小児がんを扱う我が国の臨床研究グループとして専門家間で認知されているものは表1に示した7つである。この中で日本小児白血病・リンパ腫研究グループ(JPLSG)が最も規模が大きい。小児血液腫瘍のプロトコールスタディを実施していた既存の4つの臨床研究グループ(CCLSG, JACLS, KYCCSGおよびTCCSG)がインターグループとして結集して形成されたもので、我が国の主たる小児がん治療施設のほとんどが参加している。小児血液腫瘍および血液系関連疾患に対する臨床試験11件を現在実施している(表2)。JPLSGのホームページでの組織図によると、代議員会と運営委員会が運営の中心となっており、その周囲に各種委員会、データセンター、検体センター等が配置されている。血液腫瘍以外の小児固形腫瘍については、基本的には病型ごとに研究グループが形成されている。小児の代表的な固形腫瘍である神経芽腫、横紋筋肉腫、Ewing肉腫、Wilms腫、肝芽腫については、それぞれ、JNBSG, JRSG, JESS, JWITS, JPLTのグループが形成されている。なお、小児脳腫瘍についてはJPBTCというNPOとして活動している。また、多くの研究グループは何らかの形で公的研究費の支援を受けながら活動している。治療介入型の臨床試験を実施しているグループが大半だが、ガイドライン治療を実施し基盤となる情報収集を目的とした観察研究に近い形の研究もある。

*1 国立成育医療センター研究所

**2 千葉県こども病院検査部病理科

表1 我が国の主要な小児がん臨床研究グループ

小児がん臨床研究グループ名	対象病型	実施中の試験数	ホームページなどの情報
日本小児白血病・リンパ腫研究グループ (JPLSG)	白血病, 悪性リンパ腫など	11	http://jplsg.jp
日本横紋筋肉腫研究グループ (JRSG)	横紋筋肉腫	4	文献1
日本ユウイング肉腫研究グループ (JESS)	Ewing肉腫	1	文献2
日本神経芽腫研究グループ (JNBGS)	神経芽腫	2	http://www.jnbsg.jp/
日本小児肝癌スタディグループ (JPLT)	肝芽腫など	1	http://home.hiroshima-u.ac.jp/jpltstudy/index.html
日本ウィルムス腫瘍スタディグループ (JWiTS)	Wilms腫	1	文献3
日本小児脳腫瘍コンソーシアム (JPBTC)	髄芽腫など	2	http://www.es-bureau.org/contents/consortium/

表2 現在進行中の小児がん関連臨床試験一覧

病型	試験名	研究グループ	試験ID*
急性リンパ性白血病	・乳児急性リンパ性白血病に対する早期同種造血幹細胞移植療法の有効性に関する後期第II相臨床試験 (MLL03)	JPLSG	C000000290
	・小児フィラデルフィア染色体陽性急性リンパ性白血病 (Ph+ALL) に対する imatinib mesylate 第II相臨床試験 (Ph+ALL04)	JPLSG	
急性骨髄性白血病	・小児急性前骨髄性白血病 (APL) に対する多施設共同後期第II相臨床試験 (AML-P05)	JPLSG	UMIN000000645
	・小児急性骨髄性白血病 (AML) に対する多施設共同後期第II相臨床試験 (AML-05)	JPLSG	UMIN000000511
	・ダウン症候群に発症した小児急性骨髄性白血病に対するリスク別多剤併用化学療法の後期第II相臨床試験 (AML-D05)	JPLSG	UMIN000000989
悪性リンパ腫	・ALCL99 (未分化大細胞型リンパ腫を対象としたヨーロッパとの共同研究)	JPLSG	C000000317 UMIN000000675
	・小児成熟B細胞性腫瘍に対する多施設共同後期第II相臨床試験 (B-NHL03)	JPLSG	
	・進行期小児成熟B細胞性腫瘍に対する顆粒球コロニー刺激因子 (G-CSF) の一次的予防投与の有効性に関する無作為割付比較試験 (B-NHL03 G-CSF)	JPLSG	
	・小児リンパ芽球型リンパ腫 stage I/II に対する多施設共同後期第II相臨床試験 (LLB-NHL03)	JPLSG	
・小児リンパ芽球型リンパ腫 stage III/IV に対する多施設共同後期第II相臨床試験 (ALB-NHL03)	JPLSG		
血球貪食症候群	・Treatment Protocol of the Second International HLH Study (HLH-2004)	JPLSG	
横紋筋肉腫	・横紋筋肉腫低リスクA群患者に対する短期間VAC 1.2療法の有効性および安全性の評価第II相臨床試験	JRSG	
	・横紋筋肉腫低リスクB群患者に対する短期間VAC 2.2/VA療法の有効性および安全性の評価第II相臨床試験	JRSG	
	・横紋筋肉腫中間リスク群に対するiVAC療法の有効性および安全性に関する多施設共同研究	JRSG	
	・進行性・転移性横紋筋肉腫に対する自家造血幹細胞移植療法を併用した大量化学療法第II相臨床試験	JRSG	
Ewing肉腫	・限局性ユウイング肉腫ファミリー腫瘍に対する集学的治療法の第II相臨床試験	JESS	
神経芽腫	・進行神経芽腫に対する遅延局所療法早期第II相臨床試験	JNBGS	UMIN000000973
	・高リスク神経芽腫に対する標準的治療の後期第II相臨床試験	JNBGS	UMIN000001044
肝癌	・小児肝癌に対するJPLT-2治療プロトコル臨床第II相試験	JPLT	UMIN000001116
Wilms腫	・本邦における腎腫瘍に対する病期別統一プロトコル治療の完遂率と有効性の評価 (JWiTS-2)	JWiTS	
髄芽腫またはテント上PNET	・小児髄芽腫/PNETに対する多剤併用化学療法と減量放射線療法の第II相臨床試験	JPBTC	UMIN000000545
	・乳幼児髄芽腫/PNETに対する多剤併用化学療法および大量化学療法の第II相臨床試験	JPBTC	UMIN000000546

* : 試験IDは以下のサイトで検索した。

UMIN臨床試験登録システム (UMIN CTR) : <http://www.umin.ac.jp/ctr/index-j.htm>財団法人日本医療情報センター (JAPIC)臨床試験データベース : http://www.clinicaltrials.jp/user/cte_main.jsp国立保健医療科学院臨床研究(試験)情報検索 : <http://reportal.niph.go.jp/>国立がんセンターがん情報サービス : http://ganjoho.ncc.go.jp/professional/med_info/clinical_trial/ct0120.html

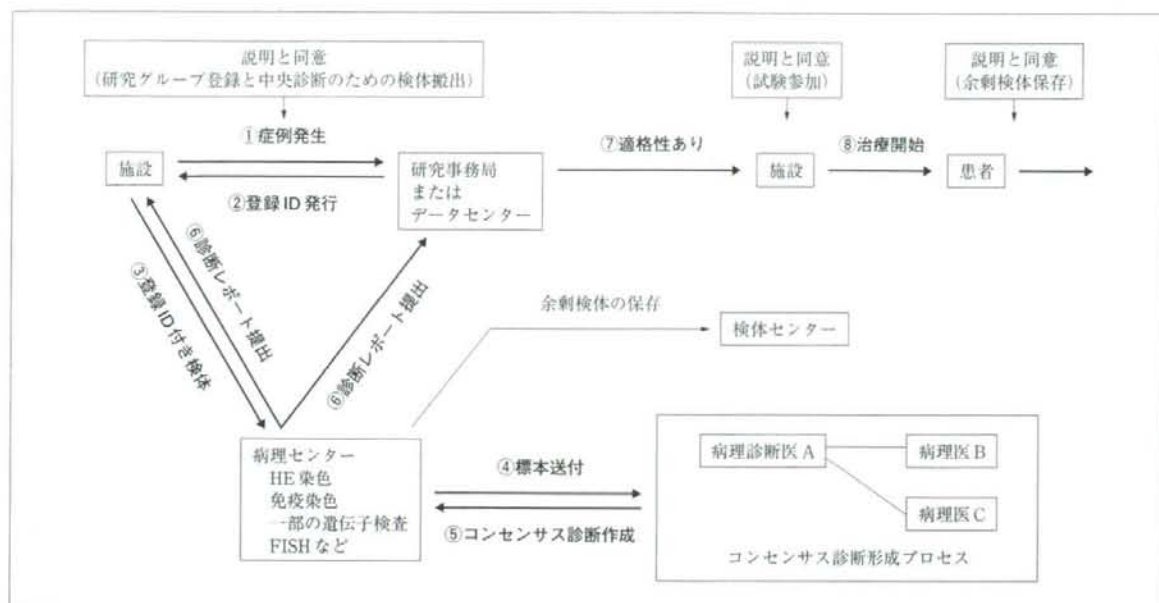


図1 小児がんの臨床試験登録と病理中央診断システム 我が国の小児がん臨床試験で一般的に行われている情報と検体の流れ、その中の病理中央診断システムと余剰検体保存の関連を示す。症例が発症した場合、施設は研究事務局あるいはデータセンターに登録申請を行い登録IDの発行を受ける(①②)。施設は患者検体に登録IDを付けて病理センターに送付する(③)。病理センターは必要な染色等を行った後、指定した病理医に標本を送付する(④)。病理医間でコンセンサス診断を作成し、病理センターを経由して診断レポートを施設ならびにデータセンターに送付する(⑤⑥)。試験参加の適格性の判断が施設に伝えられ治療が開始する(⑦⑧)。なお、このプロセスの中で、患者あるいは代諾者に対して、研究グループ登録と中央診断への検体搬出、試験参加、余剰検体保存、それぞれについて説明が行われ同意が取得される。

小児がんは稀少であるため、スタディクエスションを解決するためには、ある程度の症例数が必要となる場合がある。また、新しい臨床試験計画を独自で作成するための国内のエビデンスに乏しい場合もある。そのような場合には、海外で実施されている臨床試験に参加することも視野に入れた研究が展開されている。JPLSGが実施する試験のうち2件(ALCL99およびHLH-2004)は海外との共同研究である。

近年、臨床試験を実施するにあたっては試験内容を登録し公開することを義務づけようとする動きが高まってきている。その理由は、一般にネガティブデータは論文等で公表されない傾向があり、より透明性を確保することを目的としたものである。数年前に欧米の主要雑誌が協調し、事前に試験を登録して公開していない場合は論文掲載を行わない旨の発表を行った。以後、我が国でも登録制度と情報検索のシステムが整備されつつある。上記の研究グループが実施する臨床試験の多くが登録されており概要を検索することができる(表2脚注)。

II. 臨床研究グループと病理中央診断

さて、上記の各臨床研究グループが実施する臨床試験の多くで病理中央診断が実施されている。研究グループごとに複数の専任病理医を定めているが、その多くを日本病理学会小児腫瘍組織分類委員会のメンバーが担当している。病理中央診断の手順は試験ごとに作成される実施計画書に具体的に記載されているが、基本的には以下のごとくである(図1)。まず、試験に該当すると思われる患者が発生した場合、主治医は患者あるいは代諾者に、推測される疾患に該当する臨床試験への参加ならびに中央診断のための検体送付について説明し同意を得る。採取される検体やその処理方法は試験ごとに定められているが、病理中央診断の場合は、HE染色標本は必須で、それ以外に融合遺伝子検査などのため未固定検体の提出を求めているものもある。症例によっては免疫染色用に5~10枚程度の未染薄切標本提出を求めることもある。中央診断の

方法は一般には複数の病理医のコンセンサス診断としてレポートを作成し、標本を提出した施設ならびにデータセンター（または研究事務局）に連絡する。コンセンサス形成プロセスは研究グループごとに若干異なっている。一般には、例えば3名の診断医がいる場合、2名の診断が一致すればその診断を採用する、意見が異なれば、もう一人別の診断医の意見を求め2名の診断が一致すればそれを採用する、といった手法を採っている。意見が分かれる理由は多様である。多くの場合、標本が微量のため全体像がみえない、組織の挫滅、標本作成過程の何らかの理由による質の悪い標本などが原因になることが多いと思われる。純粋に学問的な理由、例えば、疾患概念がまだ十分に固まっておらず主観が入る余地がある、概念が確立されているが新たな指標によりさらに細分化される可能性のある場合も考えられるが、そのような場合は案外少ないと思われる。このような理由による意見の相違はむしろ歓迎すべきもので、多数例の検討でのエビデンス蓄積が重要であるし、研究グループとの連携による中央診断システムはそれらの解明を可能にするものである。

III. 小児腫瘍組織分類委員会の役割

日本病理学会小児腫瘍組織分類委員会は、日本小児外科学会、日本小児科学会からの協同の要請により設置され、1975年の小児腫瘍組織分類図譜第1篇小児肝癌、腎芽腫、神経芽腫群腫瘍の発刊をはじめとして、「癌取扱い規約」に相当する小児がんに関する分類図譜を編集・発行し、我が国における小児がんならびに関連疾患に関わる情報提供を通じて、疾患概念の認識と診断の標準化を目指すことを主たる業務としている。分類図譜はWHO分類や国際的に認知されている学術団体などが公表する最新分類に準拠し、我が国で普及させるための適切な形式に編集して定期的に発行している。以前は、「小児腫瘍組織分類図譜」という名称を使用していたが、2001年発行の版からは「小児腫瘍組織カラーアトラス」と名称変更しかつモダンなデザインの外観としている。

前述のごとく、当委員会のメンバーの多くが小児がんの臨床研究グループの中央診断担当医として参画してきたが、小児腫瘍組織分類委員会としてのまとまった活動ではなく、むしろボランティア的な活動であった。また、臨床研究グループに登録される症例は限られたものであるため、我が国の全体像を把握すること

はできないといった問題も明らかとなった（ただし、小児悪性リンパ腫の90%程度はJPLSGに登録されていると予想される）。これらの問題を解決する手段として小児腫瘍組織分類委員会が研究グループの中央診断に積極的に関与すると共に、研究に登録されない症例についても、いわばコンサルテーションのような形で中央診断できるシステム構築を現在考慮中である。このシステムを立ち上げるために、小児腫瘍中央診断委員会を小児腫瘍組織分類委員会内部に設置し、症例受付から始まる新診断システム考案、各臨床研究グループとの調整などの活動を開始した。なお、臨床試験に参加しない症例の追跡調査は重要な課題であり、それが実施可能な体制の整備をも目指している。

IV. 診断後の余剰検体や研究用検体の有効活用

言うまでもないが、正確な診断がなされ、詳細な臨床情報が付いた患者検体は研究用リソースとして極めて価値が高い。患者検体を収集する方法を考えた場合、上記のような中央診断システムを利用することが効率的かつ現実的な方法である。実際には中央診断後の残余検体（余剰検体）について患者あるいは代諾者の同意の下に研究用リソースとして保存している場合が多い（図1）。さらには、これら検体は可能な限り一箇所に集約する動きにあり、国立成育医療センター研究所や千葉県がんセンター研究所などが検体センターとして機能している。このような中央診断後の余剰検体のみならず、初めから研究用に採取され使用される検体もある。これらの検体の残余分も貴重なリソースである。現在、臨床試験に関わる余剰検体が順調に集積されてきているが、問題点としては、このような貴重なリソースをどのような取り決めて使用していくかについてのコンセンサスが未だ形成されていない点である。米国最大の小児がん研究グループであるChildren's Oncology Group (COG)では、中央診断システムならびに検体センターをコロンバスにあるNationwide Children's Hospital一箇所に集約し、また、配分ルールもグループ内でのコンセンサスとして決定している。それらも参考にしながら我が国でも共有リソースの使用ルールを決める必要がある。

V. 米国における小児がん臨床試験と中央診断、検体保存

米国では、数年前に幾つか個別に活動していた小児がん研究グループがCOGという一つの大きな枠組み

の中で活動するようになった。各種レベルの臨床試験の推進のみならず、中央診断システム構築、余剰検体の保存と活用、長期フォローアッププログラムの開発など多角的な活動を展開している。前述のようにCOGにおける中央診断と検体保存のセンターは Nationwide Children's Hospital (Columbus Children's Hospital から最近名称変更、<http://www.nationwidechildrens.org>) 内の Biopathology Center (<http://www.biopathologycenter.org>) に全て集約されている。そもそもは、同病院病理の Stephen J. Qualman 博士が始めた事業であるが、現在は極めて高度に発展したシステムとなっている (Qualman 博士は昨年引退され、Nilsa C. Ramirez 博士が後継者として就任している)。米国には1980年代より全米のがんを対象とした Cooperative Human Tissue Network (CHTN, <http://www.chtn.nci.nih.gov>) がNCIの資金により構築されており、1991年にはすでに Pediatric Division が出来上がって Columbus Children's Hospital がセンターとして指名されている。CHTNは検体を収集して中央に保存するというシステムではなく、検体は各施設で保存し情報だけを中央に集めて共有し、必要に応じて配分するというバーチャルバンキングシステムである。現在は、小児がんの多くがCOGの中で診断され治療されるため検体もCOG経由で Biopathology Center に集められるが、スタディに参加しない症例の検体も有効活用できるシステムとなっている。

COGが行う臨床試験に関わる病理中央診断についても、いったん全ての検体がCOGに集められ、必要な染色等を行ったうえで病型別に定められた病理医に送付されるという形態をとっている。なお、Biopathology CenterにはVIPER (Virtual Imaging for Pathology Education & Research, <http://vipер.epn.osc.edu/viper/>) と呼ぶバーチャルスライドユニットが存在する。オハイオ大学のスーパーコンピュータと共同で開発しており、診断そのもの、診断の標準化および教育といった目的のために活用されている。Biopathology Centerは小児がんのような稀少疾患の研究を推進するための一つの究極の形かもしれない。

VI. 小児がん登録

疾病の基本情報の収集や分析といった地道な活動は我が国では大変立ち遅れている。がん登録もその一つで、昨年成立したがん対策基本法にも盛り込まれず、

付帯事項として記載され、がん対策推進計画の中で計画の一つとして表現されるにとどまった。小児がん登録も言わずもがなの状況であり、推進計画の中には言葉としては出てくるが、小児がんを計画に盛り込んでいる自治体は皆無である。地域がん登録は2008年5月現在35道府県市で実施されているがその中で小児がん登録を意識的に位置づけているところは大阪府のみである。ただし、大阪府の場合も意識の高い小児科医の献身的な努力によって支えられているのが現状である。このような状況の中、小児がんの診療に関わる医師たちが学会ベースで小児がんの全数把握に取り組む計画を立案中である。日本小児外科学会 (<http://www.jsps.gr.jp/public/registration.htm>)、日本小児血液学会 (<http://www.jsph.info/osirase/JSPH-touroku.html>) ならびに日本小児がん学会 (<http://www.ccaj-found.or.jp/jspo/general/index.htm>) はそれぞれ独自に小児がん登録を実施してきたが、登録率の向上、国際比較の必要性などを考慮し、日本小児がん学会が関連学会と連携して従来より精度の高い小児がん登録を実施する計画を立てている。小児がんの国際比較には、International Classification of Diseases for Oncology 3rd Edition (ICD-O) に基づいた International Childhood Cancer Classification 3rd Edition (ICCC-3)⁴⁾ が使用されているため、日本小児がん学会が収集する情報を最終的にICCC-3に従って編集できるように現在使用中の登録票ならびに登録方法を改訂中である。

小児がん患者の生存率が70%ないし80%となり長期にわたる生存が期待できる状況となって、小児がん登録に求める役割に変化が起りつつある。すなわち、二次がん発生やその他の各種晩期合併症の発生をも把握できるシステムづくりを目指すべきとの意見が広まりつつある。国と自治体が連携して推進する地域がん拠点病院構想や学会主導のがん治療認定医制度や認定施設制度の定着と広がりの中で、小児がんについても成人と同じように診療体制の整備が必要であり、小児がん登録もその中に組み込まれるべきものであると考える。

おわりに

我が国における小児がんに関する質の高い臨床研究は始まったばかりと言える。病理医はこのような研究の枠組みの中でかなり重要な役割を演じる必要がある。数年間の経験からは、ある種の小児がん病型では

中央診断と施設診断の間で不一致率が10%を超えるものもあった。これらの情報をいかに現場に還元していくかは中央診断を担当する病理医ならびに小児腫瘍組織分類委員会に課せられた課題であると考え、精度の高い診断を達成するためには、医療現場の病理医の協力が必須であり、今後、学会や書物を通じて小児がんの臨床研究における病理医の活動を広く宣伝、紹介してゆきながら理解を得てゆきたいと考えている。コロンのBiopathology Centerの現責任者 Ramirez 博士との会話では、検体配分についても彼女が大変強い権限をもっていることがわかった。診断のみならず検体保存や配分に際しても病理医は強い指導力を発揮すべきなのだと思う。今後、我が国ではがん診療拠点病院のネットワークが構築されてゆくが、これらの病院では院内がん登録が義務づけられる。そのような場面でも病理医は指導的な役割を発揮するのだと思う。その際、小児がんにもご留意いただくと大変ありがたいと思う次第である。

文 献

- 1) 森川康英：小児横紋筋肉腫に対する中央病理診断及び遺伝子診断に基づく臨床試験の確立と新規治療法開発に関する研究、がん研究助成金報告書 (http://ganjoho.ncc.go.jp/pro_mhlw-cancer-grant/2005/keikaku/17-13.pdf)
- 2) 国立がんセンターがん対策情報センター：がん情報サービス、小児がんシリーズの冊子「小児のユースティング肉腫について」 (http://ganjoho.ncc.go.jp/public/qa_links/brochure/child.html)
- 3) 越永従道、七野浩之、福澤正洋：小児腎腫瘍における治療成績と方針、小児科診療 2005, 68 : 1643-1650
- 4) International Classification of Childhood Cancer, 3rd ed., SEER International Classification of Childhood Cancer (<http://seer.cancer.gov/iccc/>) を参照。また、United Kingdom Association of Cancer Registriesよりダウンロード可能 (<http://82.110.76.19/coding/iccc3.pdf>)



ORIGINAL ARTICLE

Novel risk stratification of patients with neuroblastoma by genomic signature, which is independent of molecular signature

N Tomioka^{1,2,3,11}, S Oba^{4,11}, M Ohira^{1,11}, A Misra^{2,12}, J Fridlyand⁵, S Ishii^{4,13}, Y Nakamura¹, E Isogai¹, T Hirata⁶, Y Yoshida⁷, S Todo³, Y Kaneko⁸, DG Albertson^{9,10}, D Pinkel^{9,10}, BG Feuerstein^{2,9,10,12} and A Nakagawara¹

¹Division of Biochemistry, Chiba Cancer Center Research Institute, Chiba, Japan; ²Department of Neurological Surgery, Brain Tumor Research Center, University of California, San Francisco, CA, USA; ³Department of Surgery, Hokkaido University School of Medicine, Sapporo, Japan; ⁴Graduate School of Information Science, Nara Institute of Science and Technology, Ikoma, Japan; ⁵Department of Epidemiology and Biostatistics, University of California, San Francisco, CA, USA; ⁶Hisamitsu Pharmaceutical Co. Inc., Tokyo, Japan; ⁷GENESHOT project, R&D Center, NGK Insulators, Ltd, Nagoya, Japan; ⁸Saitama Cancer Center Research Institute, Saitama, Japan; ⁹Department of Laboratory Medicine, University of California, San Francisco, CA, USA and ¹⁰Comprehensive Cancer Center, University of California, San Francisco, CA, USA

Human neuroblastoma remains enigmatic because it often shows spontaneous regression and aggressive growth. The prognosis of advanced stage of sporadic neuroblastomas is still poor. Here, we investigated whether genomic and molecular signatures could categorize new therapeutic risk groups in primary neuroblastomas. We conducted microarray-based comparative genomic hybridization (array-CGH) with a DNA chip carrying 2464 BAC clones to examine genomic aberrations of 236 neuroblastomas and used in-house cDNA microarrays for gene-expression profiling. Array-CGH demonstrated three major genomic groups of chromosomal aberrations: silent (GGS), partial gains and/or losses (GGP) and whole gains and/or losses (GGW), which well corresponded with the patterns of chromosome 17 abnormalities. They were further classified into subgroups with different outcomes. In 112 sporadic neuroblastomas, *MYCN* amplification was frequent in GGS (22%) and GGP (53%) and caused serious outcomes in patients. Sporadic tumors with a single copy of *MYCN* showed the 5-year cumulative survival rates of 89% in GGS, 53% in GGP and 85% in GGW. Molecular signatures also segregated patients into the favorable and unfavorable prognosis groups ($P=0.001$). Both univariate and multivariate analyses revealed that genomic and molecular signatures were mutually independent, powerful prognostic indicators. Thus, combined genomic and molecular signatures may categorize novel risk groups and confer new clues for

allowing tailored or even individualized medicine to patients with neuroblastoma.

Oncogene (2008) 27, 441–449; doi:10.1038/sj.onc.1210661; published online 16 July 2007

Keywords: neuroblastoma; array-CGH; molecular signature; risk stratification; microarray

Introduction

Neuroblastoma is one of the most common solid tumors in children. However, its clinical behavior is enigmatic because the tumor usually regresses spontaneously when developed in patients under 1 year of age, but often grows rapidly to cause fatal outcomes when developed as an advanced tumor in patients over the age of 1 year (Brodeur, 2003; Schwab *et al.*, 2003). Recent nationwide mass screening (MS) in Japan for discovering neuroblastoma at the age of 6 months clearly demonstrated the presence of a large number of asymptomatic tumors undergoing spontaneous regression (Woods *et al.*, 2002), which had been suggested by Beckwith and Perrin (1963). The involvement of TrkA, a high-affinity receptor for nerve growth factor, in the regression of neuroblastoma has been suggested; however, the molecular mechanisms of the regressive event still remain elusive (Nakagawara *et al.*, 1993; Nakagawara, 1998). On the other hand, the majority of sporadic neuroblastomas are discovered at advanced stages, and their prognosis is still very poor (Brodeur, 2003; Schwab *et al.*, 2003). Recently advanced cytogenetic analyses revealed that given subsets of neuroblastomas with a favorable prognosis possess the hyperdiploid karyotype of chromosomes (Look *et al.*, 1984; Tomioka *et al.*, 2003) and that the other subsets with an unfavorable prognosis usually possess the diploid or tetraploid karyotype and often have *MYCN* amplification, gains of chromosome arms 1q, 2p and 17q, as well as allelic losses of chromosome arms 1p, 3p and 11q (Brodeur,

Correspondence: Dr A Nakagawara, Division of Biochemistry, Chiba Cancer Center Research Institute, 666-2 Nitona, Chuoh-Ku, Chiba 260-8717, Japan.

E-mail: akiranak@chiba-cc.jp

¹¹These authors contributed equally to this work.

¹²Current address: Department of Neurology, Barrow Neurological Institute, St. Joseph's Hospital and Medical Center, Phoenix, AZ, USA.

¹³Current address: Graduate School of Informatics, Kyoto University, Kyoto, Japan.

Received 29 December 2006; revised 29 May 2007; accepted 11 June 2007; published online 16 July 2007

2003; Schwab *et al.*, 2003). We and other investigators have previously reported the high accuracy of gene-expression profiling to predict the prognosis of neuroblastoma (Wei *et al.*, 2004; Ohira *et al.*, 2005). However, the prognostic significance of genomic signatures when using a high-resolution DNA microarray in primary neuroblastomas has never been reported. Here, we applied microarray-based comparative genomic hybridization (array-CGH) to both sporadic and MS-detected neuroblastomas in order to comprehend their clinical behavior and found that genomic signatures, together with molecular signatures, stratified the novel risk groups in sporadic neuroblastomas.

Results

Patterns of genomic signatures in 236 primary neuroblastomas

The most prominent feature of 236 primary neuroblastomas (112 sporadic and 124 MS detected) was the apparent presence of three genomic groups (GGs) (Figure 1a, its magnified, high-resolution figures are also indicated in Supplementary Figures S1a and b): the group of few chromosomal events (silent, GGS; $n=29$); the group of partial chromosomal gains/losses (GGP; $n=77$) and the group of whole chromosomal gains/losses (GGW; $n=130$) (Supplementary Figures S2a and b). Correlation analysis revealed that the global feature (see Materials and methods) was maximally correlated with the gain of the long arm of chromosome 17 ($R=-0.807$) and with the gain of a whole chromosome 17 ($R=0.75$) (Supplementary Table S1a), therefore the genomic groups GGP and GGW were defined by the status of aberration, by 17q gain and 17 whole chromosomal gain occurred in chromosome 17, respectively. They were followed by DNA ploidy ($R=-0.642$), loss of chromosome 1p ($R=-0.521$), *MYCN* amplification ($R=-0.531$), loss of chromosome 11q ($R=-0.5$), low *TrkA* expression ($R=-0.47$) and age ≥ 1 -year old ($R=-0.466$). Even when tested in 112 sporadic tumors, the correlation coefficient was -0.773 in 17q gain, -0.705 in DNA ploidy, -0.598 in 1p loss, -0.565 in tumor stages, -0.502 in *MYCN* amplification, -0.49 in low *TrkA* expression and -0.458 in age ≥ 1 -year old (Supplementary Table S1b). These suggested that 17q gain was a characteristic and prognosis-related event in primary neuroblastomas. The percentages of DNA diploidy or tetraploidy were 83% (15/18), 66% (33/50) and 18% (17/94) in GGS, GGP and GGW tumors, respectively (Supplementary Table S2a).

GGS tumors rarely showed chromosomal aberrations except *MYCN* amplification in 5 among 29 tumors (Figure 1b, a high-resolution figure is also indicated in Supplementary Figure S1c). To date, the presence of the GGS subgroup with very silent aberrations of the tumor genome has never been verified definitely. The concern about the possible dilution of the tumor-cell DNA content by contamination of stromal cells was cleared by the detailed examination of GGS tumor specimens

(see Supplementary Figure S2b and Supplementary Information).

Seventy-seven GGP tumors, which had 17q gain, were further subgrouped computationally according to the detailed chromosomal event, the presence and/or absence of 1p loss and 11q loss, which are characteristic and *MYCN* amplification (s, single copy of *MYCN*; a, *MYCN* amplification) (Figures 1a and b, and see Supplementary Information). GGP1 tumors were characterized by 1p loss and 17q gain as main aberrations. GGP1a ($n=23$) was one of the most common GGP tumors. They showed the diploid karyotype (10/13, 77%) and had *MYCN* amplification in addition to 1p loss and 17q gain. Interestingly, GGP1s tumors lacking *MYCN* amplification ($n=6$) showed relatively frequent 2p gain, as well as 14q loss, 1q gain, 4p loss and 7p gain that were rare in GGP1a tumors with *MYCN* amplification. GGP2 tumors were characterized by the presence of both 1p loss and 11q loss, in addition to 17q gain. In GGP2a, tumors with *MYCN* amplification ($n=4$) also frequently showed 1q gain. GGP3 tumors formed a group typically characterized by the presence of 11q loss and 17q gain without 1p loss. Intriguingly, only 1 of 27 GGP3 tumors had *MYCN* amplification. All GGP4 tumors except one, which presented neither 1p loss nor 11q loss, also had no *MYCN* amplification. The percentages of diploidy/tetraploidy in GGP1, GGP2, GGP3 and GGP4 tumors were 76% (13/17), 75% (6/8), 76% (13/17) and 13% (1/8), respectively (Supplementary Table S2a).

GGW tumors with whole chromosomal gains and/or losses, especially with the predominant gain of whole chromosome 17 (Figure 1b), were mostly the tumors detected by MS (94/130, 73%; see Supplementary Table S2a). The highest incidence of MS-detected neuroblastomas was observed in GGW4s tumors that were purely composed of whole chromosomal gains/losses. The DNA ploidy analysis revealed that 82% (77/94) of GGW tumors were hyperdiploidy. Similarly to GGP tumors, GGW tumors were categorized into tumors with the following aberrations: 1p loss (GGW1, $n=5$); both 1p loss and 11q loss (GGW2, $n=2$); 11q loss (GGW3, $n=11$) and without any one (GGW4, $n=92$). GGW5 tumors ($n=20$) formed a group of tumors with a low frequency of chromosome 17 on the BAC array. Like chromosome 17, chromosomes 6 and 7 were frequently gained in GGW tumors. *MYCN* amplification was observed in only three tumors belonging to GGW4 or GGW5 (3/112, 2.7%).

Genomic signatures and clinical outcomes

Genomic signatures of neuroblastomas unveiled previously unknown relationships between genetic subgroup and patient prognosis (Figure 1b). The greatest surprise was the difference in the 5-year survival rates between the GGSa (0%, $n=5$) and GGSs (91%, $n=24$) subgroups ($P<0.001$). The other *MYCN*-amplified tumor subgroups, GGP1a ($n=23$), GGP2a ($n=4$) and GGWa ($n=3$), also showed very poor survival rates of 42, 0 and 0%, respectively. On the other hand, GGWs

neuroblastomas demonstrated good outcomes (GGW1s: 100%, $n=5$; GGW2s: 100%, $n=2$; GGW3s: 100%, $n=11$; GGW4s: 97%, $n=91$ and GGW5s: 89%,

$n=18$). The intermediate 5-year cumulative survival rates were demonstrated in GGPs tumors (GGP1s: 80%, $n=6$; GGP2s: 57%, $n=7$; GGP3s: 75%, $n=26$

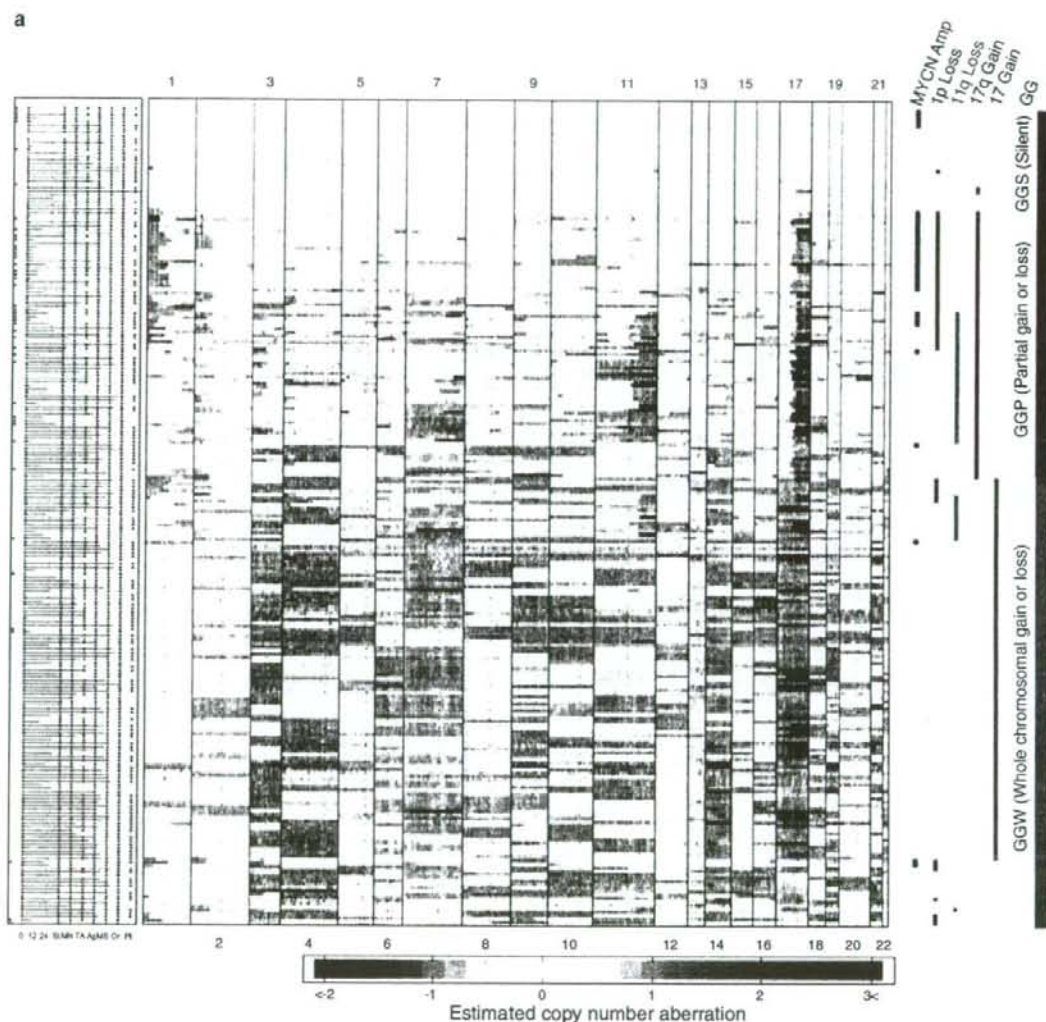


Figure 1 Genomic signatures of 236 primary neuroblastomas by array-based comparative genomic hybridization (array-CGH). (a) Overall schematic of the genomic signatures of 236 primary neuroblastomas. The left panel summarizes information about patient diagnostic factors: survival time in months after diagnosis for censored (blue bars) or dead (red bars) patients, stages 1, 2 and 4s (blue) or 3 and 4 (red) (ST), *MYCN* amplification (red) or not (blue) (MN), TrkA low (red) or high expression (blue) (TA), age more (red) or less (blue) than 12 months (Ag), sporadic tumors (red) or tumors detected by mass screening (blue) (Ms), adrenal gland (red) or others (blue) in origin (Or) and hyperploidy (blue) or diploidy/tetraploidy (red) (PI). The central panel shows estimated copy number aberrations of DNA as color matrices (blue: loss, red: gain) at chromosome locations complementary to BAC clones in each sample. The right panel shows the important features of chromosomal events, including *MYCN* amplification, deletions of chromosomes 1p and 11q, chromosome 17q gain and whole chromosome 17 gain. Furthermore, genomic groups (GGS, silent genomic group; GGP, partial chromosomal gains/losses genomic group and GGW, whole gains and/or losses genomic group) are also indicated. (b) Genomic signatures in each genomic group and the 5-year survival rates for all neuroblastomas including MS detected and sporadic tumors. Regarding each genomic group, the colored histogram represents the rates of gains and losses for each clone, where the red areas on the baseline correspond to gain and the blue areas under the baseline to loss. The right panel indicates the presence of *MYCN* amplification, 1p loss, 11q loss, 17q gain and 17 gain. The 5-year survival rates (SR) of each genomic subgroup are indicated in the right panel.

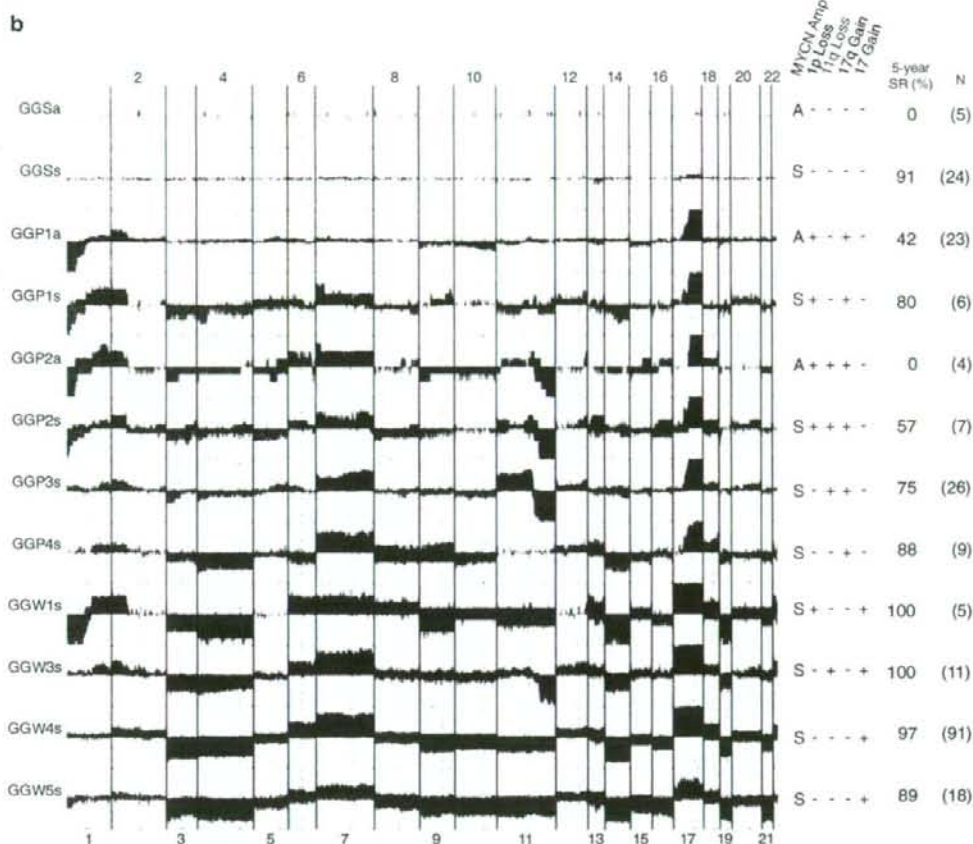


Figure 1 Continued.

and GGP4s: 88%, $n=9$). Interestingly, in GGP tumors, 1p loss (GGP1s, $n=6$) and 11q loss (GGP3s, $n=26$) seemed to have a similar effect on patient prognosis (5-year survival rates: 80 and 75%, respectively). However, GGP2s tumors with both 1p loss and 11q loss ($n=7$) had a poorer prognosis (57%) in an additive manner. Furthermore, the addition of 11q loss and 1q gain to *MYCN* amplification apparently afforded absolutely poor outcomes as suggested by the comparison between GGP1a (42%) and GGP2a tumors (0%). An analysis of 112 sporadic tumors also revealed a similar tendency except GGP1s, in which 2 sporadic tumors showed 0% survival, whereas all 4 MS-detected tumors gave good outcomes (Table 1 and Supplementary Figure S3). These suggested that *MYCN* amplification had the most powerful influence on clinical outcomes. We next compared the patterns of whole genome abnormalities of *MYCN*-amplified neuroblastomas between survivors (disease-free for more than 2 years after initiating treatment) and non-survivors (dead

of disease). One of the most striking differences was frequent loss of 11q (Supplementary Figure S4).

Effects of genomic signatures, *MYCN* amplification and age on prognosis in sporadic neuroblastomas

Figure 2 shows the Kaplan-Meier cumulative survival curves in each genetic group. In sporadic neuroblastomas, the overall survival rates of GGW, GGS and GGP were 80% ($n=36$), 68% ($n=23$) and 43% ($n=53$), respectively (Figure 2a). The prognosis of GGP was significantly poorer than that of GGW ($P=0.002$). In MS-detected tumors, on the other hand, the survival rates of GGW, GGS and GGP were 100% ($n=94$), 100% ($n=6$) and 96% ($n=24$), respectively (no significant difference among the groups; Figure 2b). The main difference between sporadic and MS-detected tumors was that the latter was detected before 1 year of age and had very few *MYCN* amplifications. Therefore, sporadic tumors were next subcategorized according

to the presence or absence of *MYCN* amplification. Figure 3a shows that the 5-year survival rates of patients with GGSs ($n=18$), GGWs ($n=33$) and GGPts ($n=25$) tumors were 89, 85 and 53%, respectively, whereas those of patients with GGSa ($n=5$), GGWa ($n=3$) and GGPa ($n=28$) tumors involving *MYCN* amplification were 0, 33 and 34%, respectively (Figure 3b). We then further examined the survival curves of patients with *MYCN*-nonamplified tumors in young (<1-year-old) and old (≥ 1 -year-old) patients. Figure 3c shows the 5-year survival rates of 88, 86 and 67% in GGWs ($n=24$), GGSs ($n=7$) and GGPts ($n=3$) tumors, respectively, among young patients, whereas they were 76, 91 and

51% in GGWs ($n=9$), GGSs ($n=11$) and GGPts ($n=22$) tumors, respectively, among old patients (Figure 3d). The former pattern was similar to that in MS-detected tumors, which had high percentages of GGW tumors, whereas the latter contained high incidences of GGP tumors.

Segregation of the prognosis of sporadic neuroblastomas with a single copy of *MYCN* by genomic and molecular signatures

Recently, we have generated a clinically useful cDNA microarray carrying 200 genes that predicts the prognosis of neuroblastomas with an accuracy rate of 89% (Ohira et al., 2005). The univariate analysis of 112 sporadic neuroblastomas showed that both genomic signatures (GGP vs GGW+GGS, $P=0.003$) and molecular signatures (posterior value <0.5 vs ≥ 0.5 , $P<0.001$) were highly significant prognostic indicators, like other variables including age ($P=0.006$), stage ($P<0.001$), tumor origin ($P=0.001$), *TrkA* expression ($P=0.004$), Shimada classification ($P<0.001$) and *MYCN* amplification ($P<0.001$; Table 2). In addition, genomic signature was a prognostic factor independent from molecular signature, age and tumor origin, although it showed no prognostic significance when stage, Shimada classification, or *MYCN* amplification was controlled (Table 2). Even in sporadic neuroblastomas with a single copy of *MYCN*, the highest significance according to the univariate analysis was given to molecular signature ($P=0.002$), followed by tumor origin ($P=0.006$) and genomic signature ($P=0.010$; Table 2). The multivariate analysis also showed that genomic signature was a prognostic indicator independent from molecular signature or tumor origin (Table 2). As shown in Figure 4, our in-house expression microarrays segregated the survival curves of patients with sporadic tumors lacking *MYCN* amplification (GGSs+GGPs+GGWs) into the favorable (94%, $n=17$) and unfavorable (42%, $n=13$) prognosis groups ($P=0.001$).

Table 1 Five-year overall survival rates of the patients with each genomic subgroup of sporadic neuroblastomas

	N	5-Year OS (%)
<i>GGS</i>		
GGSa	5	0
GGSs	18	89
<i>GGP</i>		
GGP1a	22	44
GGP1s	2	0
GGP2a	4	0
GGP2s	5	40
GGP3a	1	0
GGP3s	15	59
GGP4a	1	0
GGP4s	3	67
<i>GGW</i>		
GGW1a	0	—
GGW1s	0	—
GGW2a	0	—
GGW2s	1	100
GGW3a	0	—
GGW3s	3	100
GGW4a	1	0
GGW4s	23	87
GGW5a	2	50
GGW5s	6	67

Abbreviations: GGP, partial chromosomal gains/losses genomic group; GGS, silent genomic group; GGW, whole gains and/or losses genomic group; OS, overall survival rate.

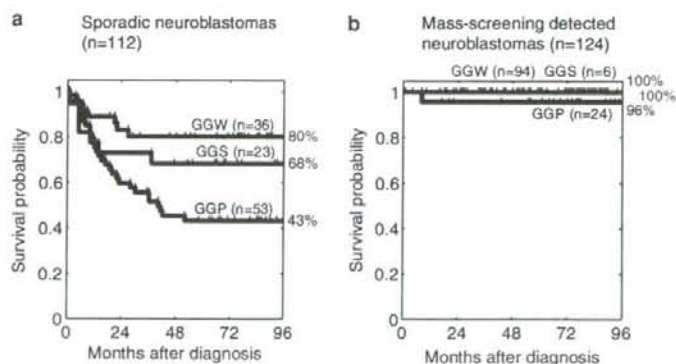


Figure 2 Kaplan Meier survival curves in three genomic groups (GGS, GGP and GGW) based on array-CGH. (a) Sporadic neuroblastomas: GGS vs GGP: $P=0.109$, GGS vs GGW: $P=0.320$ and GGP vs GGW: $P=0.002$. (b) Mass screening-detected neuroblastomas: GGS vs GGP: $P=1.000$, GGS vs GGW: $P=1.000$ and GGP vs GGW: $P=1.000$.

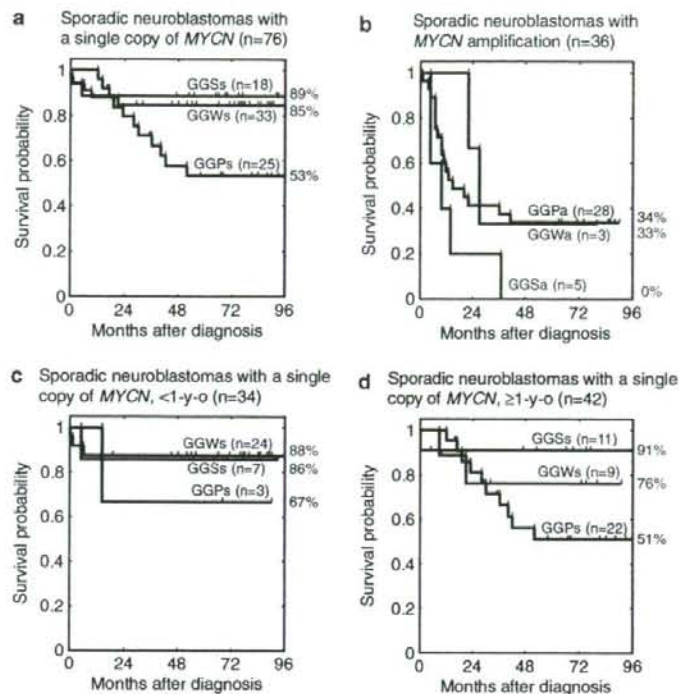


Figure 3 Kaplan Meier survival curves in three genomic groups (GGS, GGP and GGW) of sporadic neuroblastomas based on array-CGH. (a) Sporadic neuroblastomas with a single copy of *MYCN* GGS vs GGP: $P=0.035$, GGS vs GGW: $P=0.736$ and GGP vs GGW: $P=0.033$. (b) Sporadic neuroblastomas with *MYCN* amplification GGS vs GGP: $P=0.104$, GGS vs GGW: $P=0.156$ and GGP vs GGW: $P=0.642$. (c) Sporadic neuroblastomas with a single copy of *MYCN* in patients under 1 year of age GGS vs GGP: $P=1.000$, GGS vs GGW: $P=0.919$ and GGP vs GGW: $P=0.412$. (d) Sporadic neuroblastomas with a single copy of *MYCN* in patients over 1 year of age. GGS vs GGP: $P=0.063$, GGS vs GGW: $P=0.478$ and GGP vs GGW: $P=0.481$.

Discussion

The present array-CGH analysis revealed the whole feature of the genomic abnormality patterns of sporadic and MS-detected neuroblastomas. The patterns of genomic aberrations in MS-detected neuroblastomas are similar to those in sporadic tumors, suggesting that they are genetically genuine neuroblastomas which are similar to sporadic tumors found in patients under 1 year of age. Indeed, both of them have a high tendency to regress spontaneously. The exceptions we found are that the incidence of GGPs tumors is relatively higher in MS-detected tumors than in sporadic tumors found among young patients and that their clinical outcome is very good.

BAC array-based aCGH analyses have defined several minimal critical regions of gains and losses in 1p, 2p and 11q. These included minimal losses in 10 Mb regions of 1p36.3 (1pter to RP11-19901, *DIS244*) and 11q23 (from RP11-42L18 to RP11-45N4). The 2 Mb region in 1p36.2–36.3 detected by a BAC clone RP11-219F4 (*DIS507*) exhibited highest deletion frequency of 32%. By combining the expression data obtained by the

in-house microarrays harboring approximately 5340 genes derived from primary neuroblastomas, several candidate genes including *CHD5* at 1p36 (Bagchi et al., 2007) as well as *Survivin* at 17q25 (Islam et al., 2000) were identified as lowly and highly expressed genes in neuroblastomas with advanced stages, respectively (manuscript in preparation). The amplicon surrounding the *MYCN* locus was ranged from 2.4 Mb proximal (*G14110*) to 5 Mb distal (*D2S387*) of *MYCN* itself and gains were further extended to wider range, from 2pter to 2p11.

To date, the presence of the GGS subgroup with very silent aberrations of the tumor genome has never been verified definitely. The distribution of GGS tumors is very unique; namely, they are present in both MS detected and sporadic tumors removed from the patients under 1 year of age. They are also found in tumors obtained from the patients over 1 year of age, and some of them possess *MYCN* amplification. Furthermore, GGS tumors mostly show diploid karyotype. These facts suggest that GGSs tumors might represent neuroblastoma at an early stage of carcinogenesis with early oncogenic hit(s), which later develop to GGP or

Table 2 Univariate and multivariate analyses of genomic and molecular signature as well as other prognostic factors in sporadic neuroblastomas

	Sporadic NBLs (all cases)				Sporadic NBLs (MYCN, single copy)			
	N	P	HR	CI	N	P	HR	CI
Genomic signature (GGP vs GGW + GGS)	53 vs 59	0.003	2.59	(1.36, 4.90)	25 vs 51	0.010	3.41	(1.32, 8.82)
Molecular signature (posterior <0.5 vs ≥0.5)	22 vs 18	<0.001	11.15	(2.52, 49.35)	13 vs 17	0.002	14.05	(1.72, 114.89)
Age (≥1-year old vs <1-year old)	74 vs 38	0.006	2.67	(1.24, 5.77)	42 vs 34	0.070	2.47	(0.88, 6.96)
Stage (3, 4 vs 1, 2, 4s)	73 vs 38	<0.001	4.92	(1.93, 12.54)	38 vs 37	0.038	2.80	(1.00, 7.88)
Origin (adrenal vs nonadrenal)	72 vs 40	0.001	3.22	(1.43, 7.25)	41 vs 35	0.006	4.59	(1.33, 15.85)
TRKA expression (low vs high)	52 vs 36	0.004	3.37	(1.36, 8.34)	24 vs 36	0.766	1.21	(0.34, 4.31)
Shimada (unfavorable vs favorable)	39 vs 37	<0.001	4.54	(1.71, 12.07)	14 vs 36	0.668	1.37	(0.33, 5.75)
MYCN (amplification vs single copy)	36 vs 75	<0.001	3.98	(2.16, 7.35)	—	—	—	—
Genomic signature (GGP vs GGW + GGS)	15 vs 25	0.045	2.89	(1.01, 8.30)	8 vs 22	0.031	5.46	(1.09, 27.40)
Molecular signature (posterior <0.5 vs ≥0.5)	22 vs 18	0.002	7.52	(1.69, 33.38)	13 vs 17	0.034	7.41	(0.90, 60.87)
Genomic signature (GGP vs GGW + GGS)	53 vs 59	0.048	1.99	(1.05, 3.78)	25 vs 51	0.055	2.85	(1.10, 7.36)
Age (≥1-year old vs <1-year old)	74 vs 38	0.132	1.88	(0.87, 4.06)	42 vs 34	0.549	1.44	(0.51, 4.05)
Genomic signature (GGP vs GGW + GGS)	53 vs 58	0.416	1.34	(0.71, 2.54)	25 vs 50	0.098	2.61	(1.01, 6.76)
Stage (3, 4 vs 1, 2, 4s)	73 vs 38	0.005	4.06	(1.60, 10.34)	38 vs 37	0.496	1.56	(0.56, 4.40)
Genomic signature (GGP vs GGW + GGS)	53 vs 59	0.012	2.23	(1.18, 4.23)	25 vs 51	0.015	3.19	(1.23, 8.26)
Origin (adrenal vs non-adrenal)	72 vs 40	0.006	2.78	(1.24, 6.26)	41 vs 35	0.008	4.30	(1.24, 14.88)
Genomic signature (GGP vs GGW + GGS)	41 vs 47	0.079	2.17	(0.96, 4.95)	18 vs 42	0.050	3.75	(1.06, 13.33)
TRKA expression (low vs high)	52 vs 36	0.078	2.34	(0.95, 5.79)	24 vs 36	0.727	0.79	(0.22, 2.80)
Genomic signature (GGP vs GGW + GGS)	53 vs 58	0.236	1.53	(0.81, 2.90)	—	—	—	—
MYCN (amplification vs single copy)	36 vs 75	<0.001	3.30	(1.79, 6.08)	—	—	—	—

Abbreviations: CI, confidence interval; GGP, partial chromosomal gains/losses genomic group; GGS, silent genomic group; GGW, whole gains and/or losses genomic group; HR, hazard ratio; N, sample number; NBLs, neuroblastomas; P, P-value.

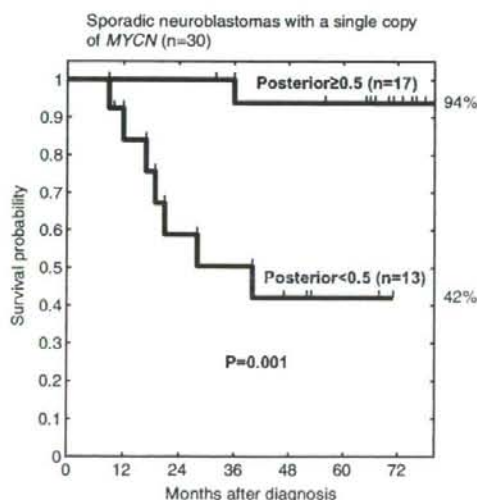


Figure 4 Kaplan Meier survival curves of sporadic neuroblastomas with a single copy of MYCN according to the molecular signature. Gene-expression profiling segregated patients into the favorable (posterior score ≥ 0.5) and unfavorable (posterior score < 0.5) prognosis groups (P = 0.001). The posterior score denotes how likely the patient would show good outcome after 5 years (Ohira et al., 2005).

GGW tumors. Since MS did not decrease the incidence of sporadic neuroblastomas (Brodeur et al., 2001; Levy, 2005), GGSs tumors in young and old patients might be

derived from different progenitor cells. It is interesting that the clinical outcome is very good for patients with MYCN-nonamplified GGSs tumors, whereas it is very bad for patients with GGSa tumors possessing MYCN amplification, implying again remarkable impact of MYCN amplification on the patient's outcome.

The GGP group is characterized by the presence of 17q gain with other chromosomal abnormalities including MYCN amplification, 1p loss and 11q loss. Since this group of tumors shows multiple chromosomal aberrations with partial gains and/or losses, unknown causes to induce genomic instability might have triggered genesis of neuroblastoma in progenitor or stem cells of sympathetic cell lineage (Maris and Matthay, 1999; Nakagawara, 2004). The frequently observed GGP tumors are as follows: GGP1a tumors with both 1p loss and MYCN amplification and GGP3s tumors with 11q loss but without MYCN amplification. The former may belong to a typical MYCN-amplified neuroblastoma (White et al., 1995) with a 5-year cumulative survival rate of 42% in our series, whereas the latter to the so-called intermediate type tumor (Srivatsan et al., 1993; Attiyeh et al., 2005) with the rate of 75%. In GGP tumors, it is obvious that MYCN amplification has the most powerful impact on the patient prognosis. Interestingly, among the GGP tumors lacking MYCN amplification, 1p loss and 11q loss seem to similarly affect the prognosis. However, GGP2s tumors with both 1p loss and 11q loss show poorer prognosis in an additive manner. The similar additive effect has also been observed in GGP1a (42%

survival) and GGP2a (0% survival) with *MYCN*-amplified tumors. These suggest that 1p loss and 11q loss may independently affect the outcomes of neuroblastoma. Interestingly, one of the main characteristics of the *MYCN*-amplified tumors found in the long-term survivors is a lack of 11q loss (Supplementary Figure S4), corresponding to the observation that the high percentage of 5-year survival rate is shown in the GGP1a group with 1p loss but without 11q loss.

GGW neuroblastoma has a favorable prognosis, as reported (Vandesompele et al., 1998). Since the pattern of chromosomal aberrations is represented by whole chromosomal gains and/or losses, mitotic dysfunction during the cell division cycle in progenitor or stem cells might have generated neuroblastoma (Maris and Matthay, 1999; Nakagawara, 2004). Interestingly, 1p loss or 11q loss in a minor population of GGWs tumors (GGW1s and GGW3s) seems not to affect the prognosis.

The presence of different patterns of genomic aberrations like GGS, GGP and GGW may reflect differences in stem or progenitor cells targeted to generate different genetic subsets of neuroblastomas. Although carcinogenic events to cause neuroblastomas may occur sequentially (Tonini, 1993), our serial analyses of six paired primary and recurrent tumors interestingly suggest that the major genetic events, for example, *MYCN* amplification, 1p loss, 11q loss and 17q gain, could occur not always in order during tumor progression (Supplementary Table S3).

Thus, the genomic signatures presented here successfully categorized new prognostic subgroups of neuroblastomas. The rather consistent patterns of genomic abnormalities provide reliable information to understanding of the genetic bases which underlie the clinical phenotypes of neuroblastomas with different survival rates. However, the pattern of genomic abnormalities may often lack biological significance affecting the clinical behavior of individual tumors. The gene-expression profile well reflects the biology of individual tumor. Therefore, establishment of the combined system of both genomic and molecular signatures is ideal for predicting the prognosis of individual patients with neuroblastoma. The present study has clearly shown that genomic and molecular signatures are independent prognostic indicators and suggests that an expression microarray could compensate for the relevant lack when used only genomic signature. In conclusion, combined genomic and molecular signatures may be clinically useful for constituting an ideal system to categorize and even individualize each tumor, which may make tailored medicine of neuroblastoma possible.

Materials and methods

Patients, tissue specimens and DN/RNA resources

Tumor specimens were collected from 236 patients who had undergone biopsy or surgery at various institutions in Japan (see Supplementary Information). They included 112 sporadic and 124 MS-detected neuroblastoma specimens. All tumors

were histopathologically diagnosed as neuroblastoma or ganglioneuroblastoma and were staged according to the International Neuroblastoma Staging System (Brodeur et al., 1993). Informed consent was obtained at each institution or hospital. The procedure of this study was approved by the Institutional Review Board of the Chiba Cancer Center (CCC7817). Patients were treated by the standard protocols (Kaneko et al., 2002; Iehara et al., 2006) in Japan between 1995 and 2003. All MS-detected tumors were diagnosed between 6 and 8 months after birth by measuring urinary catecholamine metabolites in Japan (Sawada et al., 1984). Fresh neuroblastoma tissues removed during surgery were stored at -80°C . *MYCN* copy number, *TrkA* mRNA expression and DNA ploidy were measured as reported previously (Islam et al., 2000).

Microarray-based comparative genomic hybridization

A chip carrying 2464 BAC clones prepared by ligation-mediated PCR, which covers the whole human genome at roughly 1.2-Mb resolution (Snijders et al., 2001; Albertson et al., 2003), was used. The 500-ng aliquots of tumors and reference DNAs were labeled by random priming with each Cy3-dCTP and Cy5-dCTP (Amersham Pharmacia, Piscataway, NJ, USA). Hybridization was performed as previously reported (Pinkel et al., 1998). UCSF Spot and UCSF Sproc programs to analyse values for spotted clones (Jain et al., 2002) were used. All array-CGH data are available at NCBI Gene Expression Omnibus (GEO, <http://www.ncbi.nlm.nih.gov/geo/>) with accession number GSE 5784.

cDNA microarrays

In-house cDNA microarrays, carrying 5340 cDNAs obtained from the oligo-capping cDNA libraries generated from anonymous neuroblastoma tissues (Ohira et al., 2003, 2005), were used. Preparation of RNA, hybridization, reading of spots and statistical analyses were conducted as reported previously (Ohira et al., 2005). Gene-expression profile data described in this study is available at NCBI GEO with accession number GSE 5779.

Statistical analysis

The fluorescence ratio for each array CGH spot was normalized and rescaled into estimated copy number aberrations of each clone according to the comb-fit method (Oba et al., 2006; see also Supplementary Figure S2a). Chromosomal events were detected by locally smoothing variations in copy number aberrations of clones on a chromosome and by applying threshold rules (see Supplementary Figure S2a and Supplementary Information for more detail). The numbers of whole chromosomal events, N_w and of partial chromosomal events, N_p , were counted for $22+2$ chromosomes in every specimen, and the scatter plot in the N_w - N_p plane exhibited apparent three clusters: whole differential dominant ($N_w > N_p$), partial differential dominant ($N_w < N_p$) and silent ($N_w \approx 0$, $N_p \approx 0$) (Supplementary Figure S2b). To discriminate whole differential dominant from partial differential dominant, we defined a 'global' feature variable α as computationally evaluated as the ratio between N_w and N_p ; when α was small (large), the sample was likely to be whole (partial) differential dominant (see Supplementary Information for more detail). A differential analysis of gene expression was made using standard *t*-test with the *q*-value analysis (Storey and Tibshirani, 2003) for incorporating a false discovery rate (to deal with multiple statistical tests). A survival analysis was made based on Kaplan-Meier and log-rank tests. Univariate and multivariate analyses were made according to the Cox hazard models.

Acknowledgements

We thank institutions and hospitals for providing tumor specimens (see Supplementary Information). We also thank Shigeru Sakiyama, Hiroki Nagase, Iwao Nozawa, Tadayuki Koda and technical staff, past and present, at Division of

Biochemistry, Chiba Cancer Center Research Institute. We acknowledge Hisamitsu Pharmaceutical Co. Inc., the Ministry of Education, Culture, Sports, Science and Technology of Japan, the Ministry of Health, Labour and Welfare of Japan and the Hamaguchi Foundation for the Advancement of Biochemistry for funding this work.

References

Albertson DG, Collins C, McCormick F, Gray JW. (2003). Chromosome aberrations in solid tumors. *Nat Genet* **34**: 369–376.

Attiey EF, London WB, Mosse YP, Wang Q, Winter C, Khazi D *et al*. (2005). Chromosome 1p and 11q deletions and outcome in neuroblastoma. *N Engl J Med* **353**: 2243–2253.

Bagchi A, Papazoglu C, Wu Y, Capurso D, Brodt M, Francis D *et al*. (2007). CHD5 is a tumor suppressor at human 1p36. *Cell* **128**: 459–475.

Beckwith JB, Perrin EV. (1963). *In situ* neuroblastomas: a contribution to the natural history of neural crest tumors. *Am J Pathol* **43**: 1089–1101.

Brodeur GM. (2003). Neuroblastoma: biological insight into a clinical enigma. *Nat Rev Cancer* **3**: 203–216.

Brodeur GM, Look AT, Shimada H, Hamilton VM, Maris JM, Hann HW *et al*. (2001). Biological aspects of neuroblastomas identified by mass screening in Quebec. *Med Pediatr Oncol* **36**: 157–159.

Brodeur GM, Pritchard J, Berthold F, Carlsen NL, Castel V, Castellberry RP *et al*. (1993). Revisions of the international criteria for neuroblastoma diagnosis, staging, and response to treatment. *J Clin Oncol* **11**: 1466–1477.

Iehara T, Hosoi H, Akazawa K, Matsumoto Y, Yamamoto K, Suita S *et al*. (2006). MYCN gene amplification is a powerful prognostic factor even in infantile neuroblastoma detected by mass screening. *Br J Cancer* **94**: 1510–1515.

Islam A, Kageyama H, Takada N, Kawamoto T, Takayasu H, Isogai E *et al*. (2000). High expression of Survivin, mapped to 17q25, is significantly associated with poor prognostic factors and promotes cell survival in human neuroblastoma. *Oncogene* **19**: 617–623.

Jain AN, Tokuyasu TA, Snijders AM, Segraves R, Albertson DG, Pinkel D. (2002). Fully automatic quantification of microarray image data. *Genome Res* **12**: 325–332.

Kaneko M, Tsuchida Y, Mugishima H, Ohnuma N, Yamamoto K, Kawa K *et al*. (2002). Intensified chemotherapy increases the survival rates in patients with stage 4 neuroblastoma with MYCN amplification. *J Pediatr Hematol Oncol* **24**: 613–621.

Levy IG. (2005). Neuroblastoma, ask not what your country can do for you. *J Natl Cancer Inst* **97**: 1105–1106.

Look AT, Hayes FA, Nitschke R, McWilliams NB, Green AA. (1984). Cellular DNA content as a predictor of response to chemotherapy in infants with resectable neuroblastoma. *N Engl J Med* **311**: 231–235.

Maris JM, Matthay KK. (1999). Molecular biology of neuroblastoma. *J Clin Oncol* **17**: 2264–2279.

Nakagawara A. (1998). The NGF story and neuroblastoma. *Med Pediatr Oncol* **31**: 113–115.

Nakagawara A. (2004). Neural crest development and neuroblastoma: the genetic and biological link. *Prog Brain Res* **146**: 233–242.

Nakagawara A, Arima-Nakagawara M, Scavarda NJ, Azar CG, Cantor AB, Brodeur GM. (1993). Association between high levels of expression of the TRK gene and favorable outcome in human neuroblastoma. *N Engl J Med* **328**: 847–854.

Oba S, Tomioka N, Ohira M, Ishii S. (2006). Combfit: a normalization method for array CGH data. *IPSI Trans Bioinformatics* **47**: 73–82.

Ohira M, Morohashi A, Inuzuka H, Shishikura T, Kawamoto T, Kageyama H *et al*. (2003). Expression profiling and characterization of 4200 genes cloned from primary neuroblastomas: identification of 305 genes differentially expressed between favorable and unfavorable subsets. *Oncogene* **22**: 5525–5536.

Ohira M, Oba S, Nakamura Y, Isogai E, Kaneko S, Nakagawa A *et al*. (2005). Expression profiling using a tumor-specific cDNA microarray predicts the prognosis of intermediate risk neuroblastomas. *Cancer Cell* **7**: 337–350.

Pinkel D, Segraves R, Sudar D, Clark S, Poole I, Kowbel D *et al*. (1998). High resolution analysis of DNA copy number variation using comparative genomic hybridization to microarrays. *Nat Genet* **20**: 207–211.

Sawada T, Hirayama M, Nakata T, Takeda T, Takasugi N, Mori T *et al*. (1984). Mass screening for neuroblastoma in infants in Japan. Interim report of a mass screening study group. *Lancet* **2**: 271–273.

Schwab M, Westermann F, Hero B, Berthold F. (2003). Neuroblastoma: biology and molecular and chromosomal pathology. *Lancet* **4**: 472–480.

Snijders AM, Nowak N, Segraves R, Blackwood S, Brown N, Conroy J *et al*. (2001). Assembly of microarrays for genome-wide measurement of DNA copy number. *Nat Genet* **29**: 263–264.

Srivatsan ES, Ying KL, Seeger RC. (1993). Deletion of chromosome 11 and of 14q sequences in neuroblastoma. *Genes Chromosomes Cancer* **7**: 32–37.

Storey JD, Tibshirani R. (2003). Statistical significance for genome-wide studies. *Proc Natl Acad Sci USA* **100**: 9440–9445.

Tomioka N, Kobayashi H, Kageyama H, Ohira M, Nakamura Y, Sasaki F *et al*. (2003). Chromosomes that show partial loss or gain in near-diploid tumors coincide with chromosomes that show whole loss or gain in near-triploid tumors: evidence suggesting the involvement of the same genes in the tumorigenesis of high- and low-risk neuroblastomas. *Genes Chromosomes Cancer* **36**: 139–150.

Tonini GP. (1993). Neuroblastoma: the result of multistep transformation? *Stem Cells* **11**: 276–282.

Vandesompele J, Van Roy N, Van Gele M, Laureys G, Ambros P, Heimann P *et al*. (1998). Genetic heterogeneity of neuroblastoma studied by comparative genomic hybridization. *Genes Chromosomes Cancer* **23**: 141–152.

Wei JS, Greer BT, Westermann F, Steinberg SM, Son CG, Chen QR *et al*. (2004). Prediction of clinical outcome using gene expression profiling and artificial neural networks for patients with neuroblastoma. *Cancer Res* **64**: 6883–6891.

White PS, Maris JM, Beltinger C, Sulman E, Marshall HN, Fujimori M *et al*. (1995). A region of consistent deletion in neuroblastoma maps within human chromosome 1p36.2–36.3. *Proc Natl Acad Sci USA* **92**: 5520–5524.

Woods WG, Gao RN, Shuster JJ, Robison LL, Bernstein M, Weitzman S *et al*. (2002). Screening of infants and mortality due to neuroblastoma. *N Engl J Med* **346**: 1041–1046.

Supplementary Information accompanies the paper on the Oncogene web site (<http://www.nature.com/onc>).

Expression of *TSLC1*, a candidate tumor suppressor gene mapped to chromosome 11q23, is downregulated in unfavorable neuroblastoma without promoter hypermethylation

Kiyohiro Ando¹, Miki Ohira¹, Toshinori Ozaki¹, Atsuko Nakagawa², Kohei Akazawa³, Yusuke Suenaga¹,
Yohko Nakamura¹, Tadayuki Koda⁴, Takehiko Kamijo¹, Yoshinori Murakami⁵ and Akira Nakagawara^{1*}

¹Division of Biochemistry, Chiba Cancer Center Research Institute, Chiba, Japan

²Division of Clinical Laboratory, National Center for Child Health and Development, Tokyo, Japan

³Division of Medical Information, Niigata University Medical and Dental Hospital, Niigata, Japan

⁴Center for Functional Genomics, Hisamitsu Pharmaceutical Co. Inc., Chiba, Japan

⁵Division of Molecular Pathology, Department of Cancer Biology, Institute of Medical Science, The University of Tokyo, Tokyo, Japan

Although it has been well documented that loss of human chromosome 11q is frequently observed in primary neuroblastomas, the smallest region of overlap (SRO) has not yet been precisely identified. Previously, we performed array-comparative genomic hybridization (array-CGH) analysis for 236 primary neuroblastomas to search for genomic aberrations with high-resolution. In our study, we have identified the SRO of deletion (10-Mb or less) at 11q23. Within this region, there exists a *TSLC1/IGSF4/CADM1* gene (*Tumor suppressor in lung cancer 1/Immunoglobulin superfamily 4/Cell adhesion molecule 1*), which has been identified as a putative tumor suppressor gene for lung and some other cancers. Consistent with previous observations, we have found that 35% of primary neuroblastomas harbor loss of heterozygosity (LOH) on the *TSLC1* locus. In contrast to other cancers, we could not detect the hypermethylation in its promoter region in primary neuroblastomas as well as neuroblastoma-derived cell lines. The clinicopathological analysis demonstrated that *TSLC1* expression levels significantly correlate with stage, Shimada's pathological classification, *MYCN* amplification status, *TrkA* expression levels and DNA index in primary neuroblastomas. The immunohistochemical analysis showed that *TSLC1* is remarkably reduced in unfavorable neuroblastomas. Furthermore, decreased expression levels of *TSLC1* were significantly associated with a poor prognosis in 108 patients with neuroblastoma. Additionally, *TSLC1* reduced cell proliferation in human neuroblastoma SH-SY5Y cells. Collectively, our present findings suggest that *TSLC1* acts as a candidate tumor suppressor gene for neuroblastoma.

© 2008 Wiley-Liss, Inc.

Key words: *TSLC1/IGSF4/CADM1*; neuroblastoma; 11q23; tumor suppressor

Neuroblastoma is one of the most common solid tumors in childhood and originates from the sympathoadrenal lineage of neural crest. Its biological as well as clinical behavior is highly heterogeneous in different prognostic subsets. Tumors found in patients under 1 year of age often regress spontaneously or differentiate and result in a favorable prognosis.¹ In a sharp contrast to these favorable neuroblastomas, tumors found in patients over 1 year of age are often aggressive with an unfavorable prognosis despite an intensive therapy. A large number of multiple genomic aberrations including DNA index, *MYCN* amplification status, allelic loss of the distal part of chromosome 1p and the gain of chromosome 17q have been identified in neuroblastoma.^{2,3}

Alternatively, allelic loss of 11q has been frequently observed in advanced stage of neuroblastoma with single copy of *MYCN*. Indeed, 30% of tumors harbor allelic loss of 11q, and it might be an independent prognostic indicator for clinically high-risk patients without *MYCN* amplification.^{4,5} Aberrant deletions of 11q often occur in a distal part of its long arm. Although several lines of evidence delineated the smallest region of overlaps (SRO) of deletions at 11q, it remains unclear whether there could exist a

candidate tumor suppressor gene(s) implicated in biological and clinical behaviors of neuroblastoma.^{6,7} Recently, we have performed an array-comparative genomic hybridization (array-CGH) analysis using 236 primary neuroblastomas and finally defined the SRO (10-Mb or less) at 11q23.^{3,8} During our extensive search for the already identified candidate tumor suppressor gene(s) within this region, we have found that *TSLC1/IGSF4/CADM1* gene is localized within this region.

TSLC1 gene has been originally identified as a putative tumor suppressor for non-small-cell lung cancer (NSCLC) located at chromosome 11q23 by functional complementation strategy of a human lung cancer cell line. The downregulation of *TSLC1* gene was frequently detected in various human cancers including NSCLC, prostate cancers, hepatocellular carcinomas and pancreatic cancers through its allelic loss as well as hypermethylation of its promoter region. In spite of an extensive mutation search, only 2 inactivating *TSLC1* gene mutations were detected in 161 primary tumors and tumor-derived cell lines, suggesting that *TSLC1* is rarely mutated in human cancers.⁹ *TSLC1* encodes a single membrane-spanning glycoprotein involved in cell–cell adhesion through homophilic trans interaction.¹⁰ Accumulating evidence indicates that *TSLC1* is significantly associated with biological aggressiveness and metastasis of certain types of cancer,^{11–16} whereas the functional significance of *TSLC1* in neuroblastoma remains elusive.

In the present study, we have further delineated the SRO of 11q deletion in primary neuroblastoma by array-CGH analysis and finally identified *TSLC1* gene within this region. In contrast to the other cancers, hypermethylation of *TSLC1* promoter region was undetectable in neuroblastoma. Intriguingly, the expression levels of *TSLC1* gene were highly associated with clinical stage, Shimada's pathological classification, *MYCN* amplification status, *TrkA* expression levels and DNA index in primary neuroblastoma.

Additional Supporting Information may be found in the online version of this article.

Abbreviations: array-CGH, array-comparative genomic hybridization; BAC, bacterial artificial chromosome; LOH, loss of heterozygosity; PARP, poly(ADP-ribose) polymerase; SRO, smallest region of overlap; STS, sequence-tagged-site; TSA, trichostatin A; *TSLC1*, tumor suppressor in lung cancer 1.

Grant sponsors: Ministry of Health, Labour and Welfare for Third Term Comprehensive Control Research for Cancer; Ministry of Education, Culture, Sports, Science and Technology, Japan; Scientific Research from Japan Society for the Promotion of Science.

*Correspondence to: Chiba Cancer Center Research Institute, 666-2 Nitona, Chuo-ku, Chiba 260-8717, Fax: +81-43-265-4459.

E-mail: akiranak@chiba-cc.jp

Received 21 February 2008; Accepted after revision 19 May 2008

DOI 10.1002/ijc.23776

Published online 22 August 2008 in Wiley InterScience (www.interscience.wiley.com).



Publication of the International Union Against Cancer

Material and methods

Patients, tumor specimens and cell lines

One hundred and eight tumor specimens used in the present study were kindly provided from various institutions and hospitals in Japan (see Supplementary Information). Informed consent was obtained at each institution or hospital. All tumors were diagnosed clinically as well as pathologically as neuroblastoma and staged according to the International Neuroblastoma Staging System (INSS) criteria.¹⁷ Twenty-seven patients were Stage 1, 15 Stage 2, 36 Stage 3, 23 Stage 4 and 7 Stage 4S. The patients were treated by the standard protocols as described previously.^{18,19} *MYCN* copy number, *TrkA* mRNA expression levels and DNA index were measured as reported previously.²⁰ Our present study was approved by the Institutional Review Board of the Chiba Cancer Center (CCC7817).

Human tumor-derived cell lines were cultured in RPMI 1640 medium (Nissui, Tokyo, Japan) supplemented with 10% heat-inactivated fetal bovine serum (FBS, Invitrogen, Carlsbad, CA) and 50 µg/ml penicillin/streptomycin (Invitrogen) in an incubator with humidified air at 37°C with 5% CO₂.

Array-comparative genomic hybridization

Array-CGH analysis was performed using UCSF BAC array (2464 BACs, ≈1 Mb resolution) with 236 primary neuroblastomas. Detailed experimental procedures and the criteria for losses and gains were described previously.^{3,20-22}

LOH analysis

Genomic DNA prepared from neuroblastomas and bloods was amplified by PCR-based strategy using the primer set, one of which was labeled with fluorescent dye CY5. The amplified fragments including 3 polymorphic STS markers encompassing *TSLC1*, *D11S4111*, *D11S2077* and *D11S1885*, were separated by 6% polyacrylamide gels containing 6 M urea using an automated ALF express DNA sequencer.

Semiquantitative and quantitative reverse transcription-PCR analysis

Total RNA was prepared from the indicated primary neuroblastomas, various human normal tissues and tumor-derived cell lines were subjected to semiquantitative RT-PCR using SuperScript II reverse transcriptase and random primers (Invitrogen), according to the manufacturer's instructions. Oligonucleotide primer set used to amplify *TSLC1* by semiquantitative RT-PCR was as follows: 5'-CATTTTGGAAATTTGCTGCT-3' (sense) and 5'-GGCAGCAGCAAAGAG TTTTC-3' (antisense). Quantitative real-time PCR was carried out using TaqMan(R) Gene Expression Assay System (Applied Biosystems, Foster City, CA) as described previously.²⁰ In brief, expression levels were calculated as a ratio of mRNA level for a given gene relative to mRNA for *GAPDH* in the same cDNA. The oligonucleotide primers and TaqMan probes, labeled at the 5'-end with the reporter dye 6-carboxyfluorescein (FAM) and at the 3'-end with 6-carboxytetramethylrhodamine (TAMRA), were provided by Applied Biosystems (Hs00942508_m1).

Immunohistochemistry

A 4-µm-thick section of formalin-fixed, paraffin-embedded tissues were stained with hematoxylin and eosin and the adjacent sections were immunostained for *TSLC1* using polyclonal anti-*TSLC1* antibody (CC2) as described previously.¹⁰ The BenchMark XT immunostainer (Ventana Medical Systems, Tucson, AZ) and 3-3' diaminobenzidine detection kit (Ventana Medical Systems) were used to visualize *TSLC1*. Appropriate positive and negative control experiments were also performed in parallel for each immunostaining.

Small interfering RNA

TSLC1 siRNA (GUCAAUAAGAGUGACGACUUU) and Stealth RNAi Negative Control Duplex were purchased from Sigma-Aldrich (St. Louis, MO) and Invitrogen, respectively.

Transfection

Neuroblastoma-derived SH-SY5Y cells were transfected with the indicated combinations of expression plasmids or with siRNA against *TSLC1* using LipofectAMINE 2000 or LipofectAMINE RNAiMAX transfection reagent (Invitrogen), according to the manufacturer's recommendations.

Colony formation assay

SH-SY5Y and SK-N-AS cells (1×10^5 cells/plate) were seeded in 6-well cell culture plates and transfected with or without the increasing amounts of the expression plasmid for *TSLC1* (0, 250, 750 or 1,000 ng). Total amounts of plasmid DNA per transfection were kept constant (1 µg) with the empty plasmid (pcDNA3.1-Hygro (+); Invitrogen). Forty-eight hours after transfection, cells were transferred into the fresh medium containing hygromycin (at a final concentration of 200 µg/ml) and maintained for 14 days. Drug-resistant colonies were then stained with Giemsa's solution and numbers of drug-resistant colonies were scored.

Cell growth assay

SH-SY5Y cells (6×10^5 cells/dish) were seeded in 10-cm diameter cell culture dish and transiently transfected with siRNA against *TSLC1* (240 pmol). Thirty-six hours after transfection, 2×10^6 cells were transferred into 6-well plates and transfected with 60 pmol of siRNA against *TSLC1*. At the indicated time points after transfection, number of viable cells was measured using a Coulter Counter (Coulter Electronics, Hialeah, Finland).

Bisulfite-sequencing

Sodium bisulfite-mediated modification of genomic DNA was performed using BisulFast Methylated DNA Detection Kit (Toyobo, Osaka, Japan), according to the manufacturer's instructions. Modified genomic DNA was subjected to PCR-based amplification with a primer set as described previously.²³ The PCR products containing the promoter region of *TSLC1* gene were purified by PCR Purification Kit (Qiagen, Valencia, CA) and their nucleotide sequences were determined by using a 3730 DNA Analyzer (Applied Biosystem).

Statistical analysis

Fisher's exact tests were employed to examine possible associations between *TSLC1* expression and other prognostic indicators such as age. The difference between high and low expression levels of *TSLC1* was based on the mean value obtained from quantitative real-time PCR analysis. Kaplan-Meier survival curves were calculated, and survival distributions were compared using the log-rank test. Cox regression models were used to investigate the associations between *TSLC1* expression levels, age, *MYCN* amplification status, INSS and survival. Differences were considered significant if the *p*-value was less than 0.05.

Results

Array-comparative genomic hybridization analysis identifies the smallest region of overlaps of deletion in neuroblastoma at 11q23

We have previously performed array-CGH analysis using UCSF BAC array (2464 BACs, ≈1-Mb resolution) and 236 primary neuroblastomas.³ In our array-CGH study, 66 tumors were revealed to have partial deletion of 11q as shown in Figure 1a, whose SRO were approximately 10-Mb long at 11q23 (from physical location of 110,979 to 119,806 kb in UCSC database, May 2006). To date, the data base analysis demonstrated that there could exist approximately 100 genes within this region. Of inter-

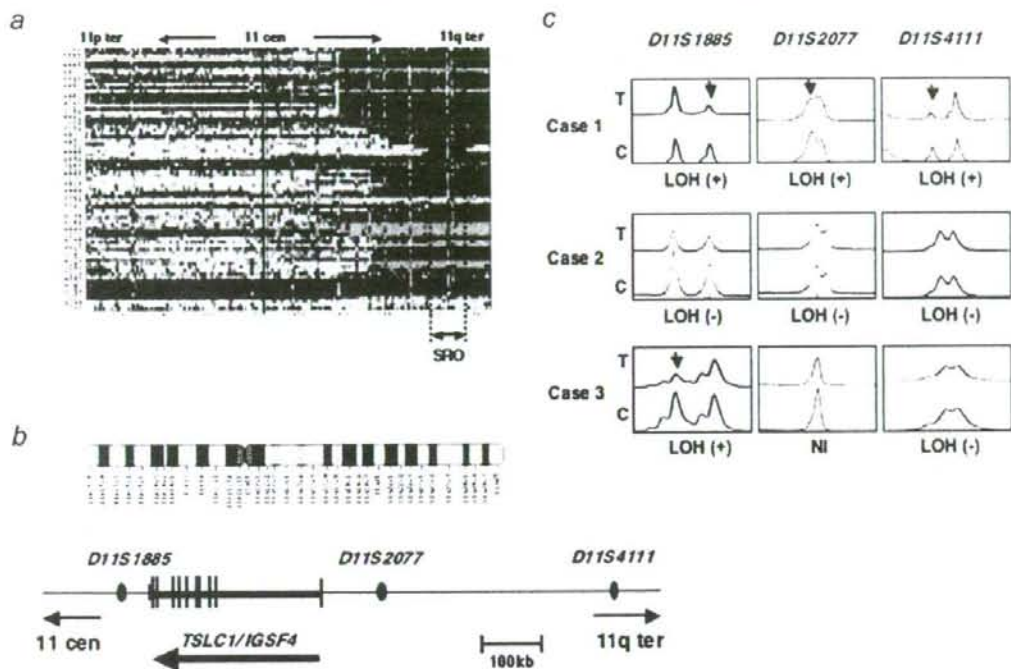


FIGURE 1 – Identification of the SRO of deletion at 11q in primary neuroblastoma. (a) Array-CGH analysis. Blue color indicates the position of the deleted area in each case. The smallest region of overlaps (SRO) of deletion at 11q is also shown. (b) The schematic drawing of the relative positions of 3 independent polymorphic markers at 11q23 used in the present study and *TSLC1* gene on human chromosome 11. (c) Representative electropherograms obtained from LOH analysis. Genomic DNA prepared from primary tumors (T) and their corresponding blood (C) was subjected to LOH analysis. Allelic losses are indicated by arrowheads. NI, not informative.

est, *TSLC1* gene which has been considered as a putative tumor suppressor for human lung as well as other cancers⁷ locates within this region (Fig. 1b). These observations prompted us to perform loss of heterozygosity (LOH) as well as expression studies of *TSLC1* gene in primary neuroblastoma.

LOH at the TSLC1 locus is frequently detected in primary neuroblastoma

According to the previous observations,^{9,24} tumor-specific downregulation of *TSLC1* gene might be largely attributed to loss of one allele in association with the hypermethylation of its promoter region in the remaining allele. To address whether LOH of *TSLC1* locus could be frequently detectable in primary neuroblastoma, we carried out LOH analysis using 3 independent fluorescently labeled polymorphic microsatellite markers (*D11S1885*, *D11S2077* and *D11S4111*) surrounding *TSLC1* gene (Fig. 1b). In accordance with the previous results,^{9,25,26} the incidence of 11q23 LOH was 22% (7 of 32) and 45% (18 of 40) in favorable neuroblastomas (Stage 1 or 2) and unfavorable ones (Stage 3 or 4), respectively (data not shown). Statistical Fisher's exact test analysis revealed that the presence of LOH at this locus is associated with unfavorable neuroblastomas ($p = 0.0493$; data not shown). It is worth noting that LOH is detectable at *D11S1885* but not at *D11S4111* in Case 3 tumor (Fig. 1c), indicating that a putative chromosome breakpoint might exist between these loci.

Downregulation of TSLC1 expression is frequently observed in unfavorable neuroblastomas

Based on the previous observations,¹¹⁻¹⁶ the expression levels of *TSLC1* were significantly reduced in advanced stages of tumors as compared with those in early stages of tumors. We then examined the expression levels of *TSLC1* in 16 favorable neuroblastomas without *MYCN* amplification and 16 unfavorable ones with *MYCN* amplification. As clearly shown in Figure 2a, *TSLC1* was expressed at lower levels in unfavorable neuroblastomas relative to favorable ones as examined by semiquantitative RT-PCR. To ask whether there could exist a possible relationship between downregulation of *TSLC1* and *MYCN* amplification, we examined the expression levels of *TSLC1* in various neuroblastoma-derived cell lines bearing single copy of *MYCN* or *MYCN* amplification. As shown in Supplementary Figure 1a, a significant downregulation of *TSLC1* expression was detected in 2 of 6 neuroblastoma cell lines carrying single copy of *MYCN* (OAN and CNB-RT) and in 4 of 21 (CHP134, KP-N-NS, SK-N-DZ and NMB) bearing *MYCN* amplification as examined by semiquantitative RT-PCR. In addition, there was no obvious correlation between the expression levels of *TSLC1* and loss of 11q except OAN, SK-N-DZ and NMB. Next, we checked the expression levels of *TSLC1* in various human adult and fetal tissues. As seen in Supplementary Figure 1b, *TSLC1* was highly expressed in normal neuronal tissues, adrenal gland, testis, prostate and liver. Our present results suggest that *TSLC1* is expressed in normal neuronal tissues and its expression levels might be regulated in a *MYCN*-dependent manner in